JACS
JOURNAL OF THE AMERICAN CHEMICAL SOCIETY

Article

pubs.acs.org/JACS

Reaction Mechanism of the Anomalous Formal Nucleophilic Borylation of Organic Halides with Silylborane: Combined Theoretical and Experimental Studies

Ryohei Uematsu,[†] Eiji Yamamoto,[‡] Satoshi Maeda,*[,§] Hajime Ito,*[,‡] and Tetsuya Taketsugu[§]

[†]Graduate School of Chemical Sciences and Engineering, [‡]Division of Chemical Process Engineering & Frontier Chemistry Center, Graduate School of Engineering, Hokkaido University, Kita-13, Nishi-8, Kita-ku, Sapporo 060-8628, Japan

[§]Department of Chemistry, Faculty of Science, Hokkaido University, Kita-10, Nishi-8, Kita-ku, Sapporo 060-0810, Japan

Supporting Information

ABSTRACT: Theoretical and experimental studies have been conducted to elucidate the mechanism of the formal nucleophilic boryl substitution of aryl and alkyl bromides with silylborane in the presence of potassium methoxide. Density functional theory was used in conjunction with the artificial force induced reaction method in the current study to determine the mechanism of this reaction. The results of this analysis led to the identification of a unique carbanion-mediated mechanism involving the halogenophilic attack of a silyl nucleophile on the bromine atom of the substrate. These calculations have, therefore, provided a mechanistic rationale for this counterintuitive borylation reaction. Furthermore, the good functional group compatibility and high reactivity exhibited by this reaction toward sterically hindered substrates can be understood in terms of the low activation energy required for the reaction of the silyl nucleophile with the bromine atom of the substrate and the subsequent rapid and selective consumption of the carbanion species by the in situ generated boron electrophile. The results of an experimental study involving the capture of the anion intermediate provided further evidence in support of the generation of a carbanion species during the course of this reaction. The anomalous formal nucleophilic borylation mechanism reported in this study could be used to provide new insights into silicon and boron chemistry.

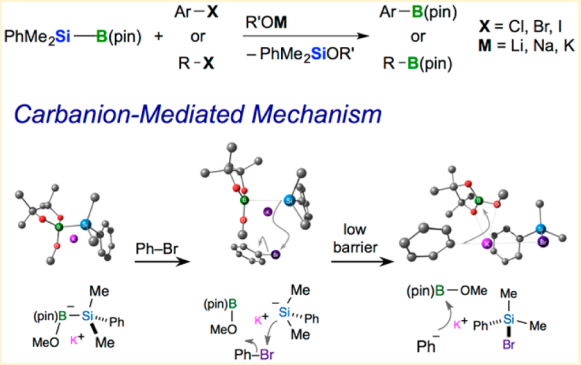

INTRODUCTION

Organoboronate esters are important building blocks in organic synthesis, and considerable research efforts have been focused on the development of synthetic methods for the construction of compounds containing this boronate ester group.[1] In this regard, Ito et al.[2] recently reported the development of a novel formal nucleophilic boryl substitution reaction, which involved the borylation of aryl, alkenyl, and alkyl halides with a silylborane species in the presence of an alkoxy base. This method of borylation is generally referred to as base-mediated borylation with a silylborane (BBS method). The BBS method shows good functional group compatibility and high levels of reactivity toward sterically hindered aryl bromides and can be conducted at ambient temperature in the absence of a transition metal catalyst. Many organometallic ate complexes (i.e., borate, silicate, cuprate, zincate, etc.) are often applied for transmetalation reactions.[3] However, one of the most interesting features of this reaction is that it appears to exhibit a counterintuitive reaction profile. For example, the reaction of a silylborane reagent with an appropriate base or nucleophile leads to the generation of a silyl nucleophile.[4] In addition, the nucleophilic aromatic substitution of aryl halides does not usually occur under low-temperature conditions without a highly electron-withdrawing group on the aromatic substrate.[5] The borylation activity described in Ito's work was, therefore, unexpected in that it deviated considerably from the reactivity behaviors previously reported in silicon and boron chemistry.[6] Although this reaction is of particular interest with regard to its synthetic utility, very little is known about the mechanism of this reaction, and further work is, therefore, required to develop a deeper understanding of the mechanism associated with this process.

Significant research efforts have been directed toward the development of borylation reactions for the synthesis of alkyl and aryl boronate esters,[7−10] and the borylation of organohalides represents one of the most reliable and widely used methods for the synthesis of organoboronate esters. Alkyl and aryl boronate esters can generally be prepared by the reaction of boron electrophiles with organolithium or Grignard reagents, which can be readily prepared from the corresponding organohalides.[7] However, the application of these reactions has been limited by their requirement for strongly basic and highly nucleophilic organometallic reagents, which invariably

Received: July 28, 2014
Published: March 15, 2015

DOI: 10.1021/ja507675f
J. Am. Chem. Soc. 2015, 137, 4090−4099

lead to poor functional group compatibility. The transition metal-catalyzed boryl substitution reaction of aryl and alkyl halides or pseudohalides has emerged as a useful alternative for the formation of organoboronate esters, showing high levels of functional group compatibility.[8,9] The application of these methods to the synthesis of pharmaceutical agents or organic materials, however, has been limited because of the costs associated with the use of transition metals on a large scale and the potential for the contamination of the product with residual transition metals.[11]

The BBS method is a newly developed, transition metal-free reaction for the synthesis of organoboronate esters, but the mechanism of this reaction has not yet been elucidated. A tentative mechanism (Scheme 1) has been proposed for this

Scheme 1. Proposed Reaction Mechanism of Formal Boryl Substitution of Organic Bromine Compounds (R = Aryl or Alkyl) with Silylborane and Alkoxy Base

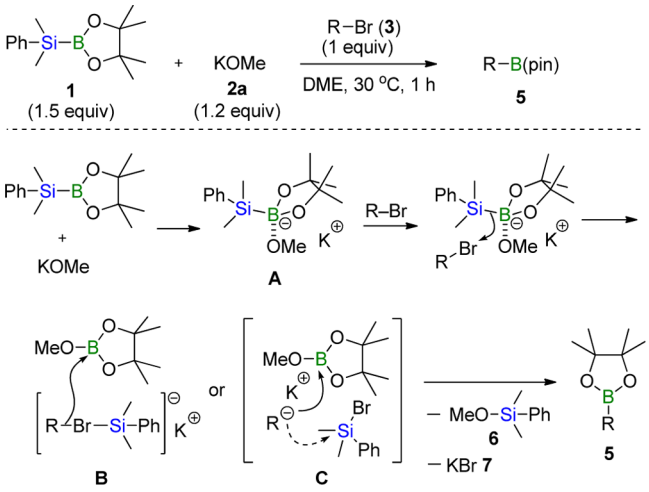

reaction based on several experimental observations,[2] which involves the formation of a carbanion species via a metal–halogen exchange.[9i,12,13] The silyl substitution reaction of aryl halides with a silyllithium reagent was also reported by Strohmann et al.[14] According to this mechanism,[2] $PhMe_2Si$–B(pin) (**1**) initially reacts with potassium methoxide (**2a**) to give silylborane/alkoxy base complex **A**. Subsequent nucleophilic attack of the silyl moiety of complex **A** on the bromine atom of alkyl or aryl bromide **3** leads to the formation of complex **B** or **C**, which contains a nucleophilic carbon moiety or carbanion species, respectively. The carbon nucleophile then attacks the boron electrophile rather than the silyl bromide (**4**) to give the corresponding organoborate intermediate $[RB(pin)OMe]^-K^+$, which provides organoboronate ester **5** through the reaction of $[RB(pin)OMe]^-K^+$ with the in situ generated silyl bromide **4**, with silyl ether **6** and potassium bromide (**7**) being formed as byproducts. There are, however, several issues with this mechanism. For example, this mechanism assumes that a thermodynamically and kinetically unstable organopotassium intermediate can be generated from a relatively unreactive silyl borate species. Furthermore, the proposed generation of a highly reactive organopotassium intermediate is not consistent with the high level of functional group compatibility observed for this method. On the basis of these inconsistencies, it is clear that further comprehensive theoretical studies are required to provide a deeper understanding of this reaction mechanism. Extensive reaction path screening could be also used to exclude other possible reaction pathways.

Given that it is not easy to explain the products resulting from the BBS method according to our current understanding of silicon and boron chemistry, it may not be possible to apply our existing theoretical understanding of the borylation of C–X and C–H bonds by transition metals[15] to this reaction. With this in mind, further studies are necessary to enhance our theoretical understanding to the extent that we can adequately explain this transformation. Nevertheless it can be difficult to apply conventional calculation methods to mechanistic studies involving novel or poorly defined reaction mechanisms because it may be necessary to consider multiple reaction pathways. Furthermore, this approach requires a large number of trial-and-error calculations to allow for the sequential identification of the intermediates and transition states (TSs) involved in the assumed mechanism. The artificial force induced reaction (AFIR) method is an automated reaction path search method[16,17] that can be used as a powerful tool in theoretical studies toward the elucidation of reaction mechanisms. The AFIR method pushes given chemical species, such as substrates, catalysts, bases, etc., together by applying an artificial force. In practice, a model function called AFIR function is used, where this function is given as the sum of the potential energy function of the reacting system and a force term. The force term eliminates potential barriers along a reaction coordinate and allows for efficient identification of product's geometry by minimization of this function. Moreover, along the minimization path of the model function (AFIR path), approximate TS geometries can be obtained. These approximate TSs are further optimized without the force in order to obtain real TSs. We note that in the following all TSs as well as minimum energy structures discussed are real TSs and local minima that were reoptimized without the force term. By systematic applications, the AFIR method allows for the identification of working reaction pathways, including unexpected ones, from the many different possibilities without the need to estimate any of the TS structures.

Herein, we present the results of a detailed density functional theory (DFT) study on the BBS method using the AFIR method. The results of this comprehensive theoretical investigation have allowed for the construction of a complete reaction pathway. This new pathway shows several similarities to the carbanion-mediated mechanism in Scheme 1. The results of this study can also be used to rationalize the selectivity of the borylation/silylation process as well as the good functional group compatibility and the high reactivity exhibited by the reactions toward sterically hindered substrates. The results of this study have also eliminated the possibility of a neutral radical or radical anion-mediated mechanism being involved in the reaction using CIS- and TDDFT-based electronic excitation energy calculations. The result of an additional experimental study for capturing the anion intermediate also supports the aryl anion-mediated mechanism.

RESULTS

Our initial efforts focused on systematically exploring the pathways potentially involved in the reaction of (dimethylphenylsilyl)boronic acid pinacol ester [$PhMe_2Si$–B(pin), **1**] with (2-bromoethyl)benzene (**3a**) in the presence of potassium methoxide using the AFIR method. Further details of this process have been provided below in the Computational Details section. On the basis of the intermediates and TSs

DOI: 10.1021/ja507675f
J. Am. Chem. Soc. 2015, 137, 4090–4099

obtained for this set of substrates, the reaction pathways for the reaction of compound **1** with bromobenzene (**3b**) in the presence of potassium methoxide were computed using standard geometry optimization calculations. These reactions are described in Scheme 2 [case-A (eq 1) and case-B (eq 2), respectively].

Scheme 2. Boron Substitution Reactions of Compounds 3a and 3b Using the BBS Method

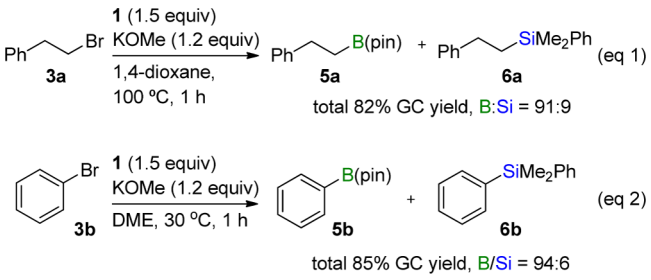

All of the structures described in this article were optimized at the M06-L[18a]/6-311+G(2d,p) level. It is important to mention that the energy profiles described in the current study have been discussed in terms of the Gibbs free energy in the gas phase. Furthermore, the free energy corrections used in the current study were estimated using ideal gas, rigid-rotor, and harmonic approximations. Single-point calculations were made at the M06[18b]/6-311+G(3df,2p) level for all of the structures identified in the current study, and solvent effects were taken into account using the C-PCM[19] method. The main features of the energy profiles discussed below do not change between these two computational levels, and information pertaining to the latter is shown in the Supporting Information.

Case-A (R = $PhCH_2CH_2$). The current mechanism was obtained by the application of a systematic reaction path search to the case-A reaction using the AFIR method.[17] The range used in the current reaction path search is described below. An approximate upper energy barrier threshold can be specified in AFIR calculations, and the value used in the current study was set to 47.8 kcal/mol (200 kJ/mol). All of the atoms in the methyl and phenyl groups of compounds **1**−**3a**, as well as the potassium atom and all the atoms in the pinacolate portion of the B(pin) moiety, were set as being inactive (i.e., reactions involving bond rearrangements in these areas of the substrates were ignored). A systematic search was then conducted at a low computational level (see Computational Details), which led to the identification of numerous reaction pathways. Reactions involving E2 elimination and α-proton elimination mechanisms with compound **3a** were found but excluded without further consideration. These reactions were not seen in the experiment[2] and were therefore considered to be unimportant to the main mechanism of the BBS method. All of the other pathways were considered at a reliable computational level, and the results are discussed below. It is important to mention that pathways for conformational changes in the inactive parts were not examined systematically.[20] Although exhaustive sampling of the conformations present in the TS is required to quantitatively predict the selectivity of a given process,[17b] this work was considered to be well beyond the scope of this study and was, therefore, not conducted.

Figure 1 shows the free energy diagram (373.15 K, 1.0 atm) obtained for the case-A reaction, which involved the borylation of an sp^3 carbon. Five elementary reactions were identified during this process, including (I) the coordination of the methoxide ion (**2a′**) to the boron atom of compound **1** to give complex $[PhMe_2Si{-}B(pin)OMe]^-K^+$ (A2 of Figure 1); (II-a) adsorption of $PhCH_2CH_2Br$ (**3a**) to A2 giving A2′; (II-b) generation of $PhMe_2Si^-$ (**8**) and MeOB(pin) (**9**) via the cleavage of the B−Si bond (A3 of Figure 1); (III) formation of $PhCH_2CH_2^-$ (**10a**) and $PhMe_2SiBr$ (**4**) by the reaction of **8** with $PhCH_2CH_2Br$ (**3a**), which allowed for the initial anion charge to be transferred from the silicon atom to the carbon atom (A4 of Figure 1); (IV) production of $[PhCH_2CH_2B(pin)OMe]^-K^+$ (**11a**) via the reaction of **9** with **10a** (A5 of Figure 1); and (V) removal of the methoxy group in **11a** by a nucleophilic substitution reaction to give the desired product, **5a** (A6 of Figure 1). We computed both paths with and without **3a** for the reaction steps (I) and (II), and Figure 1 shows only the most feasible path in which **3a** adsorbs at the step (II-a). In the steps from A3 to A5 or A7, there are also species that do not explicitly participate in the reaction, e.g., MeOB(pin) in TS(A3/A4). However, the barriers in all of these reaction steps are low. These steps thus proceed rapidly without waiting for dissociation of such species. On this point, a detailed discussion is presented for the case-B reaction in the Supporting Information.

Kleeberg et al. reported the formation of related disilyl complex $[(PhMe_2Si)_2B(pin)]^-K(18\text{-}C\text{-}6)^+$ in a reaction of 3.3 equiv of $PhMe_2Si{-}B(pin)$ and 1.0 equiv of K[(18-C-6)(O-*t*-Bu)].[4e] In our system, no obvious signal corresponding to $[(PhMe_2Si)_2B(pin)]^-$ at 9.2 ppm was observed by means of the ^{11}B NMR spectrum of the mixture of 1.5 equiv of $PhMe_2Si{-}B(pin)$ and 1.2 equiv of KOMe in DME containing 10%(v/v) of THF-d_8. The $[(PhMe_2Si)_2B(pin)]^-K(18\text{-}C\text{-}6)^+$ species was reported to have silylation reactivity, but the silylation compound was the minor product experimentally. We thus omit the reaction pathway via this species.

Silyl and alkyl anions bearing alkali metals as their counterions generally exhibit high levels of nucleophilicity and basicity, which can lead to the occurrence of various side reactions. However, the theoretical energy profile suggested that this was not the case in the current reaction. Silyl anion **8** in A3 was rapidly consumed by the subsequent halogenophilic attack process, which proceeded via TS(A3/A4′) with a very low energy barrier of only 0.4 kcal/mol. Furthermore, significant cation−π interactions existed between the potassium cation and the phenyl group of the $PhCH_2CH_2$ moiety in the metastable intermediate A4′,[21] which proceeds directly to the borylation reaction through TS(A4′/A5). Carbanion **10a** reacted with MeOB(pin) (**9**) in A4′ through TS(A4′/A5), which had a very low energy barrier of only 1.2 kcal/mol. These results therefore indicated that the reactive carbanion species were short-lived intermediates that had very little chance of reacting with the other functional groups.

Although A4 can undergo both borylation and silylation reactions, the ratio for the generation of A4 and A4′ from A3 was determined to be 23:77, based on the free energy gap of 0.9 kcal/mol between TS(A3/A4) and TS(A3/A4′) as well as the Boltzmann distribution at 373.15 K. The Boltzmann distribution revealed that the reaction path through TS(A3/A4) was the minor component and that A3 was mainly consumed by the borylation reaction, which proceeded through TS(A3/A4′) and TS(A4′/A5). The energy difference between TS(A4/A5) and TS(A4/A7) was determined to be 1.5 kcal/mol, and this value was used to predict the ratio for the generation of A5 and A7 from A4, which was 88:12. The borylation/silylation

DOI: 10.1021/ja507675f
J. Am. Chem. Soc. 2015, 137, 4090−4099

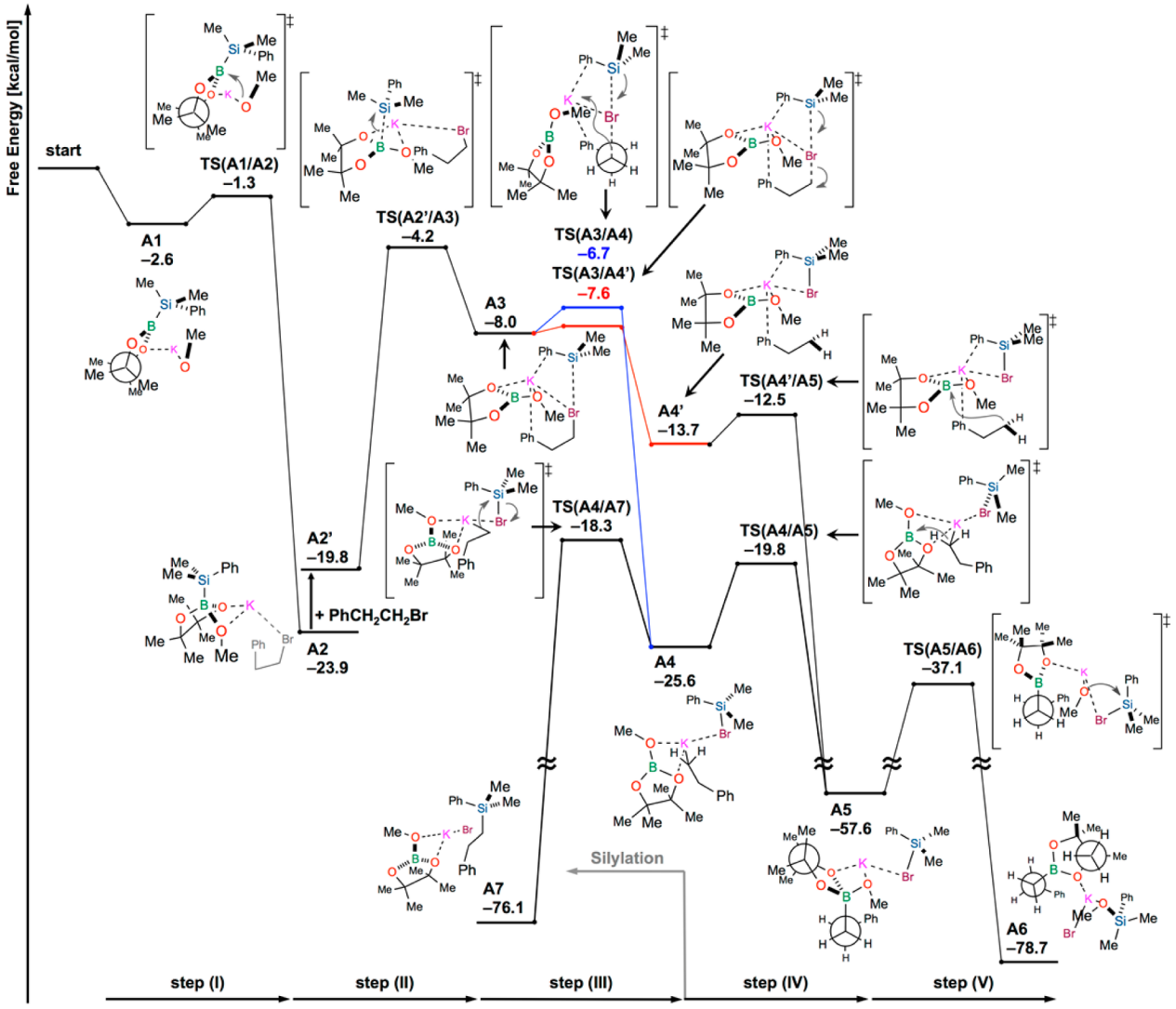

Figure 1. Reaction pathways leading to the boron product. "Start" corresponds to the reactant (i.e., **1**, **2a**, and **3a**, which were separately optimized), A*n*, to an intermediate complex (local minimum),[20] and TS(A*n*/A*m*), to the transition state connecting A*n* and A*m*. Gibbs free energy values (373.15 K, 1.0 atm) based on M06-L/6-311+G(2d,p) calculations relative to the start position are shown in kcal/mol. Schematic representations of the optimized structures corresponding to A*n* or TS(A*n*/A*m*) are shown in the current reaction. For steps from the start position to A2, profiles without **3a** are presented as the most reasonable path.

ratio was then calculated by combining the two ratios described above for the two different branches of the reaction and was found to be 97:3. This ratio was, therefore, consistent with the experimental borylation/silylation selectivity of 91:9.[2]

In the final step, $[PhCH_2CH_2B(pin)OMe]^-K^+$ (**11a**) reacts with $PhMe_2SiBr$ (**4**) in A5. Although there was a substantial energy barrier to this step, there is no need to discuss this step in greater detail because the desired product was obtained from both A5 and A6 following an aqueous quench of the reaction. Of the five different reaction steps, step (II), which involved a heterolytic B−Si bond cleavage reaction, had the highest energy barrier and was, therefore, considered to be the rate-determining step in this reaction.

The possibility of the silyl substitution via an S_N2 mechanism in the case-A reaction system was investigated. The combination of a silylborane species with a strong base can lead to the in situ production of nucleophilic silyl species.[4] With this in mind, it was envisaged that $PhMe_2Si^-$ (**8**) could react with compound **3a** via an S_N2 pathway.[2] The AFIR search identified a reaction path corresponding to this S_N2 mechanism. Two alternative S_N2 pathways leading to the formation of C−O bonds were also identified during the AFIR search, and TSs for all three of these S_N2 pathways are described in Figure 2. The free energies ($\Delta G^{\ddagger}$) relative to the individually optimized reactants ("start" in Figure 1) are shown below each TS structure together with the activation free energies ($\Delta\Delta G^{\ddagger}$). The nucleophilic attack of the methoxide group through the TSs shown in Figure 2a,b would require the formation of unstable TSs with high $\Delta G^{\ddagger}$ values of 15.6 and 22.4 kcal/mol, respectively. The TS for the silylation, which would involve the nucleophilic attack of $PhMe_2Si^-$ (**8**), in Figure 2c was also found to be unfavorable, with a $\Delta G^{\ddagger}$ value of −0.1 kcal/mol, which was higher than that of the TSs shown in Figure 1. Furthermore, the activation barriers ($\Delta\Delta G^{\ddagger}$) for these pathways were also high. On the basis of these results, the S_N2 pathways were dismissed as having a negligible impact on the outcome of the current reactions.

Case-B (R = Ph). The free energy diagram (303.15 K, 1.0 atm) for the borylation and silylation reactions of the sp^2 carbon in the case-B reaction is shown in Figure 3. It is noteworthy that

DOI: 10.1021/ja507675f
J. Am. Chem. Soc. 2015, 137, 4090−4099

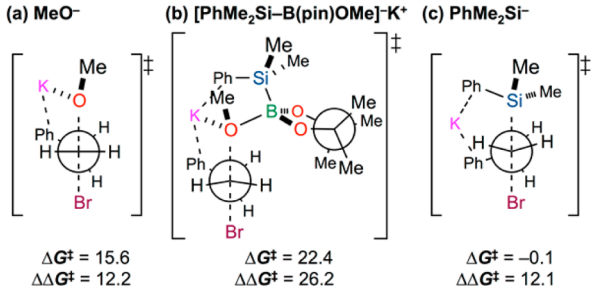

Figure 2. TS structures, free energies ($\Delta G^{\ddagger}$) relative to the reactants (i.e., **1**, **2a**, and **3a**), and activation free energies ($\Delta\Delta G^{\ddagger}$) of the S_N2 reaction pathways. Free energy values (373.15 K, 1.0 atm) based on M06-L/6-311+G(2d,p) calculations are given in kcal/mol. It was assumed that the molecule that did not participate in the reactions in (a) and (c) existed at an infinity distance.

different temperatures of 373.15 and 303.15 K were used to evaluate the free energy profiles for the case-A and case-B reactions, respectively, to allow for the results to be compared with experimental results that were obtained at the same temperatures. Figure 3 looks very similar to the diagram shown in Figure 1 in that the overall reaction is composed of five steps (i.e., steps I–V), which were discussed above for the case-A reaction. Given that the final step was considered to have very little impact on the outcome of the overall reaction, the rate-determining step was, therefore, determined to be the step corresponding to the cleavage of the B–Si bond through TS(B2′/B3).

Detachment/attachment of PhBr (**3b**) at B3 is slower than the forward and backward steps. This was confirmed by evaluation of the free energy along their reaction coordinates. That is, we performed a constrained optimization fixing the distance between Br in **3b** and K in the remaining part at R_{K-Br} = 6 Å and the normal-mode analysis for the projected Hessian. This gave an estimate of the free energy of −3.4 kcal/mol at R_{K-Br} = 6 Å. This is higher than both TS(B3/B4) and TS(B2′/B3). On the other hand, the free energy at R_{K-Br} = 6 Å along

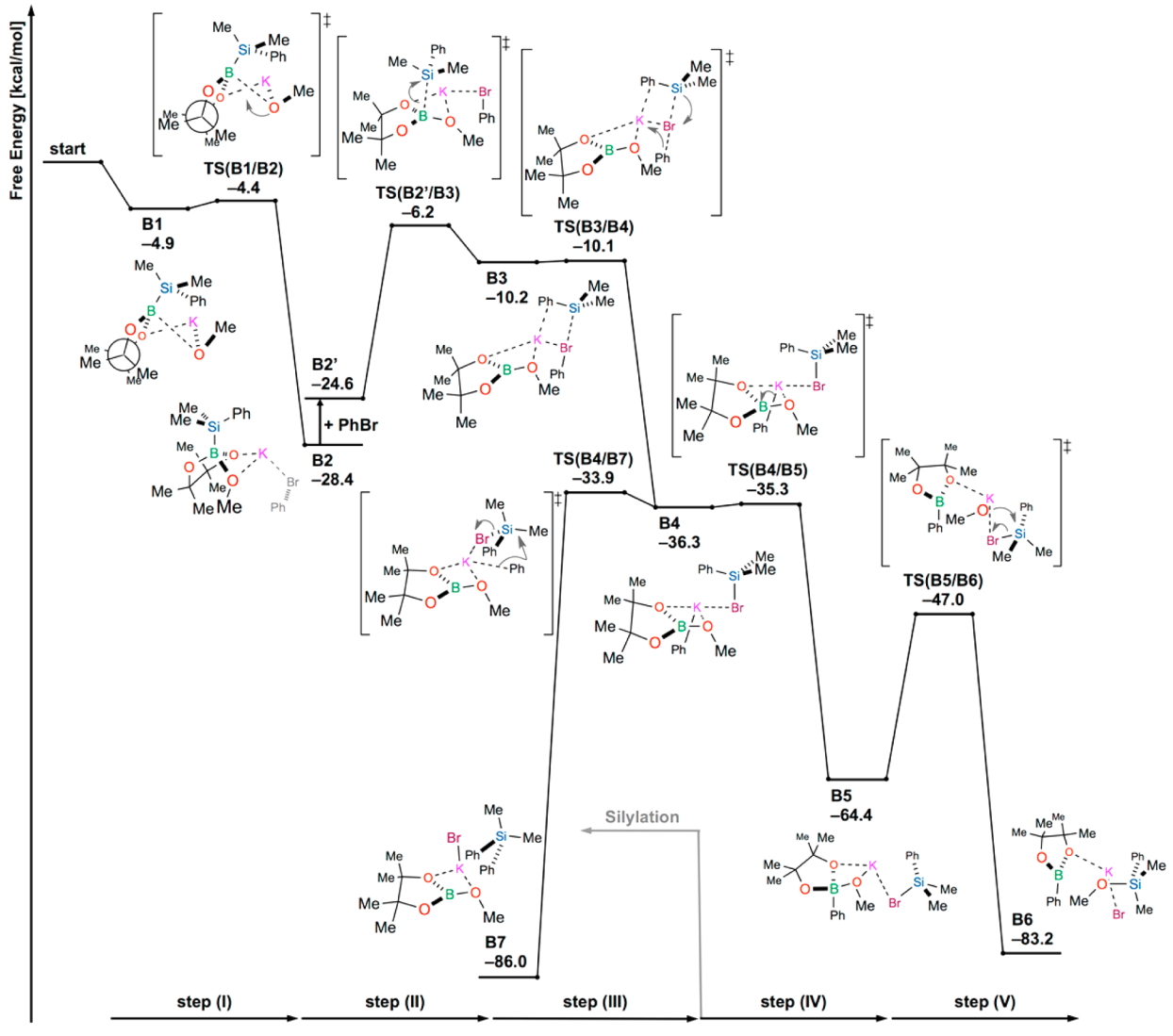

Figure 3. Reaction pathways leading to the B/Si products. "Start" corresponds to the different reactants (i.e., **1**, **2a**, and **3b**, which were optimized separately). B*n* refers to an intermediate complex (local minimum),[20] and TS(B*n*/B*m*), to a transition state connecting B*n* and B*m*. Gibbs free energy values (303.15 K, 1.0 atm) based on M06-L/6-311+G(2d,p) calculations relative to the start position are presented in kcal/mol. Schematic representations of the optimized B*n* and TS(B*n*/B*m*) structures in the current reaction. For steps from the start position to B2, profiles without **3b** are presented as the most reasonable path.

DOI: 10.1021/ja507675f
J. Am. Chem. Soc. 2015, 137, 4090–4099

the detachment/attachment coordinate of **3b** at B2′ was −20.9 kcal/mol. This is much lower than TS(B2′/B3). The profile shown in Figure 2 thus is the best path concerning existence or nonexistence of **3b**. Details of this analysis are described in Supporting Information Figures S4, S6-1, and S6-2.

Decomposition of reaction complexes with dissociation of species that do not directly participate in the reaction can be a favored process. However, this is not the case in the reaction steps from B3 to B5 and B7 of the present reaction. This is because activation free energies required in these steps are all very low. In other words, these steps proceed rapidly before dissociation of such species. In order to confirm this, we calculated free energy values along dissociation coordinates of these species. For example, for reaction complex B4, the distance R_{K-B} between the K atom and the B atom in (pin)B−OMe was chosen as the dissociation coordinate of (pin)B−OMe. Then, we performed a constrained optimization, fixing the distance at R_{K-B} = 8 Å and the normal-mode analysis for the projected Hessian. This gave an estimate of the free energy of −27.0 kcal/mol at R_{K-B} = 8 Å. This is much higher than the TSs for the forward reactions: −35.3 kcal/mol for borylation and −33.9 kcal/mol for silylation. Thus, the reaction proceeds before dissociation of (pin)B−OMe. In this way, we confirmed that the reaction proceeds with the path from B3 to B5 and B7 shown in Figure 3 without dissociation of any species. Details of this analysis are described in Supporting Information Figure S6-1.

The possibility of radical reaction pathways was checked using several calculations. Strohmann et al.[14a] suggested the existence of a radical-mediated pathway in the reaction of silyl anions with organic halides, which is mechanistically related to the BBS method,[14a] and TS(B3/B4), which involves the halogenophilic attack step, that could possess some radical character. The results of a CIS-based MO stability check[22] at the UM06-L/6-311+G(2d,p) level, however, indicated that TS(B3/B4) was closed-shell at the electronic ground state. Furthermore, TDDFT-based electronic excitation energy calculations for the complex composed of B2 and PhBr revealed that the closed-shell electronic ground state was well separated from the first electronic excited state by 103.6 and 122.2 kcal/mol at the CAM-B3LYP[23]/6-311+G(2d,p) and LC-BLYP[24]/6-311+G(2d,p) levels, respectively. These results therefore excluded the possibility of an open-shell radical species being involved in this reaction.

A significant difference was found between the case-A and case-B pathways in terms of the complexes containing the anionic intermediates $PhCH_2CH_2^-$ and Ph^- (A4′ and B4). In the case-B reaction, cleavage of the C−Br bond resulted in the formation of the stable intermediate B4 bearing a K−C bond. The interaction between the terminal C atom of the $PhCH_2CH_2^-$ anion and the potassium cation in A4′ was weakened, however, by the strong interaction between the potassium cation and the Ph group, which separated the potassium cation from the terminal C atom. The relatively strong interaction between the potassium cation and the Ph group of the $PhCH_2CH_2^-$ anion could explain why the metastable intermediate A4′ was identified as a local potential energy minimum in the case-A reaction.

In a similar manner to the case-A reaction, the case-B reaction also involved two reaction pathways at B4 (i.e., borylation and silylation reactions). Experimental results showed that the borylation reaction occurred in preference to the silylation reaction. This preference can be understood in terms of the difference in the free energy values of TS(B4/B5) and TS(B4/B7), with the former being 1.4 kcal/mol lower in energy than the latter. This energy difference was very similar to the corresponding energy gap of 1.5 kcal/mol in the case-A reaction. Taken together, these results indicated that the borylation reaction was kinetically favored over the silylation reaction. On the basis of this free energy gap and the Boltzmann distribution, the B/Si branching ratio of the case-B reaction was estimated to be 92:8, and this ratio was consistent with the experimental borylation/silylation ratio of 94:6 from the BBS method.

Experimental Results. The validity of the proposed aryl anion-mediated mechanism was supported by the results of an experiment involving the borylation of an aryl halide (**3c**) bearing a TBS ether group next to its bromine atom (Scheme 3a). The

Scheme 3. Intramolecular Retro-Brook Rearrangement of a Silylborane Species in the Presence of an Alkoxy Base

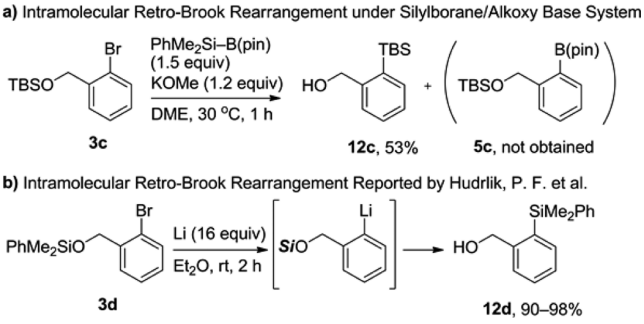

reaction of **3c** with silylborane **1** in the presence of potassium methoxide proceeded as an intramolecular silyl substitution reaction instead of a boryl substitution reaction to give TBS-substituted product **12c** in moderate yield (53% isolated yield), without detection of borylation product **5c**. This result suggested that the corresponding aryl anion species was generated in situ and that this species subsequently attacked the silicon atom of the proximal TBS group at a greater rate than the boron or phenyldimethylsilyl electrophile derived from the silylborane. It is noteworthy that Hudrlik et al.[25] recently reported an intramolecular retro-Brook rearrangement, which proceeded via a similar mechanism (Scheme 3b).

Substrate and Base Dependence. We now have the major reaction path for the BBS method. Thus, it would be interesting to look at energy profiles of this path for different substrates and bases. In practice, five aryl halides, **3e**−**3i**, and four bases, **2b**−**2e**, listed in Scheme 4 were considered. In the

Scheme 4. Aryl Halides and Bases Used in Discussions on the Reactivity of the BBS Method

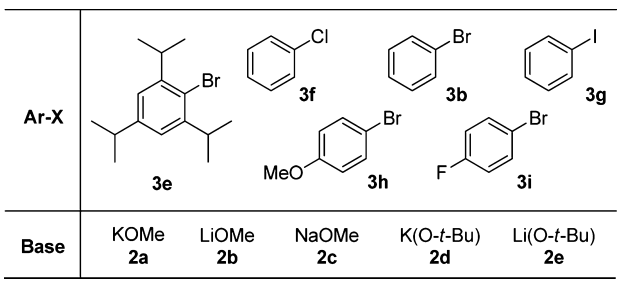

Supporting Information, all computed energy profiles are compared in Figure 3. Some trends seen in these energy

DOI: 10.1021/ja507675f
J. Am. Chem. Soc. 2015, 137, 4090−4099

profiles provided several points that can be beneficial for further optimization of the BBS method.

At first, the activation energy in the halogenophilic attack on sterically hindered 2,4,6-triisopropylbromobenzene (**3e**) was investigated and found to be reasonably low ($\Delta\Delta G^{\ddagger}$ = 1.9 kcal/mol, Figure 4). TS(B2′/B3) was slightly lower than TS(B3/B4) for **3e**

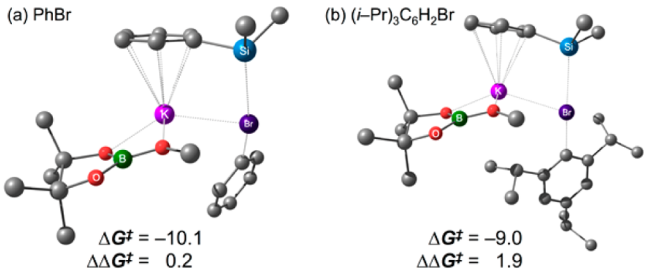

Figure 4. TS structures, free energies ($\Delta G^{\ddagger}$) relative to the reactants (**1**, **2a**, and **3b**/**3e**), and activation free energies ($\Delta\Delta G^{\ddagger}$) for the halogenophilic attack reaction steps. Free energy values (303.15 K, 1.0 atm) based on M06-L/6-311+G(2d,p) calculations are given in kcal/mol.

as shown in Figure S5-1, and the reaction thus is expected to proceed smoothly with **3e**. This is consistent with the high reactivity of the BBS method toward sterically hindered substrates.[2]

Second, the halide effect [PhBr (**3b**) vs PhCl (**3f**) vs PhI (**3g**)] and substitution effect of *para* position [PhBr (**3b**) vs *p*-MeO−C_6H_4Br (**3h**) vs *p*-F−C_6H_4Br (**3i**)] were investigated experimentally and theoretically (see the Supporting Information: S11 for experimental data and Figures S5-2, S5-4, S6-2, and S6-3 for theoretical energy profiles.) Experimentally, it was shown that the reactivity increases as **3g** > **3b** > **3f** and **3i** > **3b** > **3h**.[26] These experiments also showed that reactions of different substrates are in competition when two substrates are combined together. Consistently, $\Delta G^{\ddagger}$ values at the rate-determining TS(B2′/B3) are very close to each other for these substrates; $\Delta G^{\ddagger}$ values at TS(B2′/B3) are 7.5, 8.7, 7.3, 6.9, and 7.2 kcal/mol for **3b**, **3f**, **3g**, **3h**, and **3i**, respectively, in our best estimate with inclusion of the solvent effect by C-PCM. These values reproduce the experimental reactivity trends qualitatively; only the $\Delta G^{\ddagger}$ for **3h** showed deviation from the experimental trend. Nevertheless, these <1 kcal/mol energy differences are too small to be discussed with the present computational level. Moreover, the computational trend changed by inclusion of the solvent effect with C-PCM (see Supporting Information). Treatment with more accurate ab initio theory and explicit consideration of movements of surrounding solvent molecules are required for further quantitative predictions.

Third, the impact of the base is investigated. We reported that KOMe (**2a**) gave the borylation and minor silylation products of *p*-MeO−C_6H_4Br (**3h**) in 92% yield with high B/Si ratio (95:5). The reaction with NaOMe (**2c**) resulted in 81% yield (**5b** + **6b**) with a B/Si ratio of 80:20. We also found that the borylation of PhBr (**3b**) with K(O-*t*-Bu) (**2d**) and Li(O-*t*-Bu) (**2e**) as the base gave moderate to high yield and B/Si selectivity [66% yield (**5b** + **6b**), B/Si = 73:27; 94% yield (**5b** + **6b**), B/Si = 85:15, respectively] under previously reported reaction conditions.[2] Theoretical results showed that all of the bases shown in Scheme 4 provide $\Delta\Delta G^{\ddagger}$ values that are low enough to promote the borylation reaction. However, it is difficult to fully elucidate the reactivity and selectivity trends of the experimental results. This is probably because of the solubility difference of the bases (for details, see Figure S10 in the Supporting Information). KOMe (**2a**), LiOMe (**2b**), and NaOMe (**2c**) are only partially soluble in dimethoxyethane, whereas K(O-*t*-Bu) (**2d**) and Li(O-*t*-Bu) (**2e**) are fairly soluble in the solvent. It is noteworthy that the reaction of LiOMe (**2b**) afforded no borylation/silylation products in the experiment, although the theoretical results for LiOMe indicate its moderate reactivity. This inconsistency is attributable to the very slow Si−B bond cleavage in the real LiOMe reaction system because of the extremely low solubility of LiOMe in the reaction medium and relatively higher $\Delta\Delta G^{\ddagger}$ value at the Si−B bond cleavage step (B2′ → B3) (for details, see the Supporting Information). Furthermore, in this study, we optimized TSs obtained for the reaction with **2a** after substituting the corresponding metal atom without further conformational analysis. The B/Si selectivity would be determined by a subtle energy gap between the silylation TS and the borylation TS, and its quantitative prediction further requires an extensive conformational sampling. Such an analysis for quantitative discussions of the B/Si selectivity will be a future subject.

■ DISCUSSION

The pathways computed in the current study for the case-A and case-B reactions provide adequate explanations of many of the characteristic features of the BBS method. The BBS method was initially highlighted for its good functional group compatibility and high reactivity toward sterically hindered substrates.[2] In the reaction profiles shown in Figures 1 and 3, the step involving the cleavage of the Si−B bond through TS(A_{or}B2′/A_{or}B3) was identified as the rate-determining step. The reaction proceeded rapidly beyond this point, with unstable intermediates such as the silyl anion and carbanion species being immediately consumed with very low energy barriers (see the steps from A_{or}B3 to A_{or}B5 in Figures 1 and 3). This result indicated that all of these intermediates almost exclusively underwent the borylation reaction, even when they contained other reactive functional groups. Furthermore, the structures of the TSs involved in these steps provide some rationale for the high borylation reactivity observed in the BBS method toward sterically hindered aryl bromides. The TS(B3/B4) structure shows that the steric hindrance provided by the substrate would be too far removed from the reactive σ^*(C−Br) orbital to have a noticeable impact on the reactivity, whereas catalysts usually interact with the carbon and bromo atoms in the C−Br bond directly in the transition metal-catalyzed boryl substitution of aryl bromides. Actually, a bulky substrate **3e** showed a reasonable potential profile with low barriers.

The BBS method proceeded to give a product with a counterintuitive borylation reaction as well as a small amount of the silylation product (5−10%).[2] This distribution of products suggests that these two channels are competing with each other and that the energy barrier for the borylation reaction must be slightly lower than that of the silylation reaction by a few kcal/mol. This feature of the BBS method was effectively reproduced in the current reaction profiles. Furthermore, the results of simple thermodynamic analyses on the basis of their free energy barriers and Boltzmann distributions predicted borylation/silylation ratios of the case-A and case-B reactions to be 97:3 and 92:8, respectively. These ratios were qualitatively consistent with the experimental ratios of 91:9 and 94:6. The energy profiles for these reactions showed that all of the

DOI: 10.1021/ja507675f
J. Am. Chem. Soc. 2015, 137, 4090−4099

borylation/silylation TSs existed along favorable pathways [i.e., TS(A4′/A5), TS(A4/A5), TS(A4/A7), TS(B4/B5), and TS(B4/B7)], with energy barriers in the range of 1−7 kcal/mol. These low energy barriers were attributed to the carbanion species, $PhCH_2CH_2^-$ and Ph^-, which are highly reactive intermediates that can react spontaneously with B or Si. The B/Si selectivities observed in these reactions can be understood, therefore, in terms of the effectiveness of their interorbital attraction between the Ph^- and B/Si species. The selectivity of an organic transformation can be understood and controlled in terms of the hard and soft acids and bases principle. With this in mind, the sp^3/sp^2 hybrid orbital of $PhCH_2CH_2^-/Ph^-$ would better overlap much more effectively with the empty 2p orbital of the MeOB(pin) moiety than the σ^*(Si−Br) orbital of the $PhMe_2SiBr$ moiety. This would explain why carbanions prefer to react with B rather than Si.

The results of the current experiment strongly suggest that several carbanion species were generated *in situ*, and these results, therefore, support the involvement of unstable intermediate A4, A4′, or B4 in the reaction. Taken together with the comparison of the experimental observations and theoretical reaction profiles provided above, these findings provide strong support for the proposed mechanism shown in Scheme 1.[2] Furthermore, the application of the current AFIR search to the case-A reaction allowed for the contributions from many other possible pathways to be eliminated in a systematic way, which provided further evidence in support of the validity of this mechanism. Although the mechanism shown in Scheme 1 may look unusual in the sense that it involves highly reactive intermediates derived from silyl anion and carbanion species, it is important to realize that all of the theoretical and experimental results of the current study are consistent with this mechanism.

■ CONCLUSIONS

A theoretical investigation of the BBS reaction has been conducted using the AFIR method. The resulting complete reaction pathway for the BBS method was shown to involve the halogenophilic attack of a silyl anion on the bromine atom of the substrate and the rapid and selective consumption of a resulting carbanion species by a boron electrophile. These calculations provided a rational explanation for the counter-intuitive borylation reactivity as well as accounted for the good functional group compatibility of the reaction and its high reactivity toward sterically hindered substrates. The use of the AFIR method in the current study not only provided a complete reaction pathway but also demonstrated the validity of the proposed reaction mechanism by comprehensively accounting for the other reaction mechanisms. An experiment was also conducted involving the capture of an aryl anion intermediate, and the results of this experiment provided further support for the generation of a carbanion species during the reaction. It is hoped that this novel mechanism will allow us to expand our knowledge and understanding of silicon and boron chemistry.

■ COMPUTATIONAL DETAILS

For the case-A reaction, reaction pathways involving the conversion of the reactants (i.e., **1**, **2a**, and **3a**) to the major products and byproducts were searched systematically at the B3LYP[27] level with small basis sets (STO-3G for all of the methyl and phenyl groups and 6-31G for all of the other groups) using the AFIR method. It is necessary to determine an upper threshold for the energy barrier when the AFIR method is being used to conduct a systematic reaction pathway search. The upper threshold used in the current study was set to 47.8 kcal/mol (200 kJ/mol) for the initial searches. These searches can be performed efficiently by choosing the reactive sites appropriately. Three reactive sites were defined in reactants for the case-A reaction, including (i) the ethylene moiety and Br atom in $PhCH_2CH_2Br$, (ii) the B and Si atoms in $PhMe_2Si$−B(pin), and (iii) the O atom in potassium methoxide. These settings were employed consistently in all of the reaction steps. The AFIR method gives many approximate reaction pathways, called AFIR paths, as minimization pathways of the AFIR function.[16] The AFIR paths at the low computational level were subsequently optimized using a conventional path optimization method known as the locally updated planes[28] (LUP) method at the M06-L/6-311+G(d) level. Because the AFIR path can provide a good estimate of the minimum energy path, LUP calculations converge quickly, and only five LUP iterations were considered. Peaks along the LUP paths were then optimized to the true TSs at the M06-L/6-311+G(d) level. Important pathways were further optimized at the M06-L/6-311+G(2d,p) level, and free energy corrections in the gas phase were estimated by assuming ideal gas, rigid-rotor, and harmonic approximations. Natural population analysis was performed at the M06-L/6-311+G(2d,p) level. TSs for the case-B reaction were optimized using important TSs obtained from the case-A reaction by substituting the $PhCH_2CH_2$ group for a Ph group. Moreover, for discussions of the substrate and base dependences, these TSs were further optimized at the same computational level with different substrates and bases, where, only for I atom, the Stuttgard ECP46MDF[29] effective core potential and corresponding basis set were applied. All of the DFT calculations were performed with the Gaussian 09 suite of programs.[30] Automated searches as well as geometry optimizations were performed using a developmental version of the GRRM program with the DFT gradients and Hessians.[31]

Single-point calculations were performed at the M06/6-311+G(3df,2p) level for all of the local minima and TSs shown in Figures 1 and 3 and TS(B2′/B3) shown in Figure S5-2 and S5-4. These solvent effects were considered using the C-PCM method.[19] 1,4-Dioxane was selected in the C-PCM calculations because it was the experimentally optimized solvent in the case-A reaction. THF was selected as the solvent for the case-B reaction in the C-PCM calculations because the C-PCM parameters for THF were available in Gaussian 09. Furthermore, experimental results have demonstrated that THF exhibits similar reactivity and selectivity properties as those of dimethoxyethane, which was employed as the optimized solvent in the experiment. Gas-phase free energy corrections were conducted at the M06-L/6-311+G(2d,p) level and added to the C-PCM single-point energies at the M06/6-311+G(3df,2p) level to allow for the free energy values to be estimated. In the case-A and case-B reactions, the free energy profiles from $A_{or}B2$ to $A_{or}B5$ in the C-PCM solvents did not differ significantly from those in the gas-phase calculations. Most notably, the reaction steps following TS($A_{or}B2/A_{or}B3$) to $A_{or}B5$ possessed negligible barriers, which remained unchanged regardless of any solvent effects. The free energy profiles in the C-PCM-solvents are shown in the Supporting Information.

■ EXPERIMENTAL SECTION

General. All of the materials used in the current study were obtained from commercial suppliers and purified using standard procedures unless otherwise noted. $PhMe_2Si$−B(pin) was synthesized according to the reported procedures[32] or provided by Frontier Scientific, Inc. Dry solvents for the reaction were purchased from commercial suppliers and used as received unless otherwise noted. DME was distilled from sodium benzophenone ketyl prior to use. KOMe (95%) was purchased from Sigma-Aldrich (St. Louis, MO, USA) and used as supplied without further purification. NMR spectra were recorded on a JEOL JNM-ECS400 spectrometer (JEOL, Tokyo, Japan). ^{1}H, ^{13}C, and ^{11}B NMR spectra were obtained at 400, 100, and 127 MHz, respectively. Tetramethylsilane (^{1}H), $CDCl_3$ (^{13}C), and $BF_3{\cdot}Et_2O$ (^{11}B) were employed as reference standards in the ^{1}H, ^{13}C,

DOI: 10.1021/ja507675f
J. Am. Chem. Soc. 2015, 137, 4090−4099

^{11}B NMR experiments, respectively. 1,4-Diisopropylbenzene was used as the internal standard for determining GC yield. The reaction shown in eq 2 was performed in accordance with the previously reported conditions on a 0.2 mmol scale.[2] The reaction of phenyl bromide with $PhMe_2Si$–B(pin) and Li(O-*t*-Bu) was also conducted according to the previously reported procedures using Li(O-*t*-Bu) instead of KOMe.[2] Elemental analysis and high-resolution mass spectra were recorded at the Center for Instrumental Analysis, Hokkaido University. Compound **3c** was prepared according to reported procedures.[1,33]

Procedures for Intramolecular Retro-Brook Rearrangement with Silylborane and an Alkoxy Base. Potassium methoxide (42.1 mg, 0.6 mmol) was added to a vial in a glovebox under an atmosphere of argon, and the vial was then sealed with a screw cap containing a silicon-coated rubber septum. The reaction vial was removed from the glovebox and connected to a vacuum/nitrogen manifold through a needle. DME (5 mL) and (dimethylphenylsilyl)-boronic acid pinacol ester (196.7 mg, 0.75 mmol) were then added to the vial, and the resulting mixture was stirred for 10 min at 30 °C. Aryl bromide **3c** (150.7 mg, 0.50 mmol) was then added to the reaction mixture in a dropwise manner via a syringe, and the resulting mixture was stirred for 1 h at 30 °C. The reaction mixture was then passed through a thin pad of silica-gel, and the filtrate was collected and evaporated to dryness to give a crude product as a residue, which was purified by silica-gel column chromatography using 1–15% (v/v) hexane/Et_2O as the eluent to give crude product **12c** (63% NMR yield). The product was contaminated with a small amout of $PhMe_2SiOH$, which was removed under reduced pressure (0.3–0.4 hPa) at 45 °C. The resulting crude product **12c** was further purified by sublimation to give **12c** in 53% yield (55.5 mg, 0.266 mmol) as a white solid.

Characterization of the Retro-Brook Rearrangement Product 12c. *[2-(tert-Butyldimethylsilyl)phenyl]methanol (**12c**).*

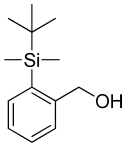

^{1}H NMR (392 MHz, $CDCl_3$, δ): 0.36 (s, 6H), 0.88 (s, 9H), 4.73 (s, 2H), 7.26 (dt, J = 1.1, 7.4 Hz, 1H), 7.38 (dt, J = 1.4, 7.5 Hz, 1H), 7.45–7.53 (m, 2H). ^{13}C NMR (99 MHz, $CDCl_3$, δ): −3.2 (CH_3), 17.6 (C), 26.8 (CH_3), 65.8 (CH_2), 126.5 (CH), 127.8 (CH), 129.4 (CH), 135.2 (C), 136.2 (CH), 146.6 (C). HRMS-APCI (m/z): $[M - H]^+$ calcd for $C_{13}H_{21}OSi$, 221.13672; found, 221.13670. Anal. Calcd for $C_{13}H_{22}OSi$: C, 70.21%; H, 9.97%. Found: C, 69.96%; H, 10.10%.

Experimental Procedure for in Situ ^{11}B{^{1}H} NMR Analysis of KOMe Adduct of $PhMe_2Si$–B(pin). In a glovebox filled with argon, KOMe (8.4 mg, 0.12 mmol) was added into a reaction vial with a screw cap. After the vial was sealed with a silicon-coated rubber septum, the vial was removed from the glovebox and connected with a nitrogen glass manifold through a needle. After dry DME (0.9 mL) and dry THF-d_8 (0.1 mL) were added, the mixture was preheated at 30 °C with stirring. Then, $PhMe_2Si$–B(pin) (39.3 mg, 0.15 mmol) was added to the solution and stirred for 10 min. The mixture was then transferred into a boron free, quartz NMR sample tube under nitrogen. Then, the ^{11}B{^{1}H} NMR spectrum was recorded at room temperature.

■ ASSOCIATED CONTENT

Supporting Information

(S1) Full reference for Gaussian 09, (S2) energy profiles including solvent effects estimated by C-PCM, (S3) energy profiles in terms of electronic energy + zero point vibration energy, (S4) pathways from start to silyl potassium intermediate with explicit participation of **3a**/**3b**, (S5) substrate and base dependence, (S6) free energy values along coordination/decoordination coordinates, (S7) natural population analysis (S8) Cartesian coordinates of the structures shown in Figures 1–4 and S4–S6, (S9) ^{1}H and ^{13}C NMR spectra of **12c**, (S10) appearance of a DME solution of KOMe or KOMe and $PhMe_2Si$–B(pin), and (S11) results and representative procedures for competing reactions of aryl halides. This material is available free of charge via the Internet at http://pubs.acs.org.

■ AUTHOR INFORMATION

Corresponding Authors

*(S.M.) smaeda@mail.sci.hokudai.ac.jp

*(H.I.) hajito@eng.hokudai.ac.jp

Notes

The authors declare no competing financial interest.

■ ACKNOWLEDGMENTS

This work was supported in part by a grant from the Japan Society for the Promotion of Science (Grants-in-Aid for Scientific Research (KAKENHI) no. 23685004 at Hokkaido University), JSPS KAKENHI grant no. 26·2447, and a Sasakawa Scientific Research Grant from the Japan Science Society for the Promotion of Science. Calculations were performed using computational resources at the Academic Center for Computing and Media Studies (ACCMS) of Kyoto University and the Research Center for Computational Science at the National Institute of Natural Sciences (NINS). A research fellowship for young scientists was awarded to R.U. by the Institute for Quantum Chemical Exploration (IQCE). A part of $PhMe_2Si$–B(pin) was provided by Frontier Scientific, Inc.

■ REFERENCES

(1) (a) Miyaura, N.; Suzuki, A. *Chem. Rev.* **1995**, *95*, 2457–2483. (b) *Boronic Acids: Preparation and Applications in Organic Synthesis, Medicine and Materials*, 2nd ed.; Hall, D. G., Ed.; Wiley-VCH: Weinheim, Germany, 2011.

(2) Yamamoto, E.; Izumi, K.; Horita, Y.; Ito, H. *J. Am. Chem. Soc.* **2012**, *134*, 19997–20000.

(3) (a) Nishikata, T.; Yamamoto, Y.; Miyaura, N. *Organometalics* **2004**, *23*, 4317–4324. (b) Nakao, Y.; Hiyama, T. *Chem. Soc. Rev.* **2011**, *40*, 4893–4901. (c) Wilf, P. *Synthesis* **1993**, *6*, 527–557.

(4) (a) O'Brien, J. M.; Hoveyda, A. H. *J. Am. Chem. Soc.* **2011**, *133*, 7712–7715. (b) Ito, H.; Horita, Y.; Yamamoto, E. *Chem. Commun.* **2012**, *48*, 8006–8008. (c) Kawachi, A.; Minamimoto, T.; Tamao, K. *Chem. Lett.* **2001**, 1216–1217. (d) Hata, T.; Kitagawa, H.; Masai, H.; Kurahashi, T.; Shimizu, M.; Hiyama, T. *Angew. Chem., Int. Ed.* **2001**, *40*, 790–792. (e) Borner, C.; Kleeberg, C. *Eur. J. Inorg. Chem.* **2014**, 2486–2489.

(5) Clayden, J.; Greeves, N.; Warren, S. *Organic Chemistry*, 2nd ed.; Oxford University Press: Oxford, 2012.

(6) Oestreich, M.; Hartmann, E.; Mewald, M. *Chem. Rev.* **2013**, *113*, 402–441.

(7) (a) Brown, H. C.; Cole, T. E. *Organometallics* **1983**, *2*, 1316–1319. (b) Brown, H. C.; Srebnik, M.; Cole, T. E. *Organometallics* **1986**, *5*, 2300–2303. (c) Baron, O.; Knochel, P. *Angew. Chem., Int. Ed.* **2005**, *44*, 3133–3135. (d) Clary, J. W.; Rettenmaier, T. J.; Snelling, R.; Bryks, W.; Banwell, J.; Wipke, W. T.; Singaram, B. *J. Org. Chem.* **2011**, *76*, 9602–9610. (e) Pintaric, C.; Olivero, S.; Gimbert, Y.; Chavant, P. Y.; Duñach, E. *J. Am. Chem. Soc.* **2010**, *132*, 11825–11827.

(8) For recent reviews of transition metal-catalyzed borylation of aryl halides, see: (a) Chow, W. K.; Yuen, O. Y.; Choy, P. Y.; So, C. M.; Lau, C. P.; Wong, W. T.; Kwong, F. Y. *RSC Adv.* **2013**, *3*, 12518–12539. (b) Primas, N.; Bouillon, A.; Rault, S. *Tetrahedron* **2010**, *66*, 8121–8136. (c) Ishiyama, T.; Miyaura, N. *Chem. Rec.* **2004**, *3*, 271–280.

(9) For selected recent papers on transition metal-catalyzed borylation of aryl halides, see: (a) Ishiyama, T.; Murata, M.; Miyaura, N. *J. Org. Chem.* **1995**, *60*, 7508–7510. (b) Ito, H.; Kubota, K. *Org. Lett.* **2012**, *14*, 890–893. (c) Kubota, K.; Yamamoto, E.; Ito, H. *J. Am. Chem. Soc.* **2013**, *135*, 2635–2640. (d) Bose, S. K.;

DOI: 10.1021/ja507675f
J. Am. Chem. Soc. 2015, 137, 4090–4099

Fucke, K.; Liu, L.; Steel, P. G.; Marder, T. B. *Angew. Chem., Int. Ed.* **2014**, *53*, 1799−1803. (e) Dudnik, A. S.; Fu, G. C. *J. Am. Chem. Soc.* **2012**, *134*, 10693−10697. (f) Yi, J.; Liu, J.-H.; Dai, J.-J.; Yang, C.-T.; Fu, Y.; Liu, L. *Adv. Synth. Catal.* **2012**, *354*, 1685−1691. (g) Murata, M.; Watanabe, S.; Masuda, Y. *Tetrahedron Lett.* **2000**, *41*, 5877−5880. (h) Zhang, P.; Roundtree, I. A.; Morken, J. P. *Org. Lett.* **2012**, *14*, 1416−1419. (i) Nagashima, Y.; Takita, R.; Yoshida, K.; Hirano, K.; Uchiyama, M. *J. Am. Chem. Soc.* **2013**, *135*, 18730−18733. (j) Kleeberg, C.; Dang, L.; Lin, Z.; Marder, T. B. *Angew. Chem., Int. Ed.* **2009**, *48*, 5350−5354.

(10) For recent reviews of transition metal-catalyzed C−H borylation, see: (a) Hartwig, J. F. *Acc. Chem. Res.* **2012**, *45*, 864−873. (b) Mkhalid, I. A. I.; Barnard, J. H.; Marder, T. B.; Murphy, J. M.; Hartwig, J. F. *Chem. Rev.* **2010**, *110*, 890−931.

(11) Rosso, V. W.; Lust, D. A.; Bernot, P. J.; Grosso, J. A.; Modi, S. P.; Rusowics, A.; Sedergran, T. C.; Simpson, J. H.; Srivastava, S. K.; Humora, M. J.; Anderson, N. G. *Org. Process Res. Dev.* **1997**, *1*, 311−314.

(12) For studies of the metal−halogen exchange mechanism concerning halogenophilic attack of boryl nucleophiles, see: Cheung, M. S.; Marder, T. B.; Lin, Z. *Organometallics* **2011**, *30*, 3018−3028.

(13) For related halogen−metal exchange reactions, see: (a) Mori, M.; Kaneta, N.; Isono, N.; Shibasaki, M. *Tetrahedron Lett.* **1991**, *32*, 6139−6142. (b) Ando, K. *J. Org. Chem.* **2006**, *71*, 1837−1850. (c) Beak, P.; Allen, D. J. *J. Am. Chem. Soc.* **1992**, *114*, 3420−3425. (d) Harada, T.; Katsuhira, T.; Oku, A. *J. Org. Chem.* **1992**, *57*, 5805−5807. (e) Farnham, W. B.; Calabrese, J. C. *J. Am. Chem. Soc.* **1986**, *108*, 2449−2451. (f) Rogers, H. R.; Houk, J. *J. Am. Chem. Soc.* **1982**, *104*, 522−525. (g) Winkler, H. J. S.; Winkler, H. *J. Am. Chem. Soc.* **1966**, *88*, 969−974. (h) Winkler, H. J. S.; Winkler, H. *J. Am. Chem. Soc.* **1966**, *88*, 964−969.

(14) (a) Däschlein, C.; Bauer, S. O.; Strohmann, C. *Eur. J. Inorg. Chem.* **2011**, 1454−1465. (b) Strohmann, C.; Bindl, M.; Fraaß, V. C.; Hörnig, J. *Angew. Chem., Int. Ed.* **2004**, *43*, 1011−1014.

(15) For recent examples of computational study of transition metal-catalyzed boryl substitution of haloarenes and arene C−H borylation, see: (a) Liu, B.; Gao, M.; Dang, L.; Zhao, H.; Marder, T. B.; Lin, Z. *Organometallics* **2012**, *31*, 3410−3425. (b) Dang, L.; Lin, Z.; Marder, T. B. *Organometallics* **2010**, *29*, 917−927. (c) Zhao, H.; Dang, L.; Marder, T. B.; Lin, Z. *J. Am. Chem. Soc.* **2008**, *130*, 5586−5594. (d) Abe, Y.; Kuramoto, K.; Ehara, M.; Nakatsuji, H.; Suginome, M.; Murakami, M.; Ito, Y. *Organometallics* **2008**, *27*, 1736−1742. (e) Dang, L.; Lin, Z.; Marder, T. B. *Organometallics* **2008**, *27*, 4443−4454. (f) Dang, L.; Zhao, H.; Lin, Z. *Organometallics* **2008**, *27*, 1178−1186. (g) Dang, L.; Zhao, H.; Lin, Z.; Marder, T. D. *Organometallics* **2007**, *26*, 2824−2832. (h) Lam, K. C.; Lin, Z.; Marder, T. B. *Organometallics* **2007**, *26*, 3149−3156. (i) Zhao, H.; Lin, Z.; Marder, T. B. *J. Am. Chem. Soc.* **2006**, *128*, 15637−15643. (j) Hartwig, J. F.; Cock, K. S.; Hapke, M.; Incarvito, C. D.; Fan, Y.; Webster, C. E.; Hall, M. B. *J. Am. Chem. Soc.* **2005**, *127*, 2538−2552. (k) Lam, W. H.; Lam, K. C.; Lin, Z.; Shimada, S.; Perutz, R. N.; Marder, T. B. *Dalton Trans.* **2004**, 1556−1562. (l) Sumimoto, M.; Iwane, N.; Takahama, T.; Sakaki, S. *J. Am. Chem. Soc.* **2004**, *126*, 10457−10471. (m) Webster, C. E.; Fan, Y.; Hall, M. B.; Kunz, D.; Hartwig, J. F. *J. Am. Chem. Soc.* **2003**, *125*, 858−859. (n) Tamura, H.; Yamazaki, H.; Sato, H.; Sakaki, S. *J. Am. Chem. Soc.* **2003**, *125*, 16114−16126. (o) Lam, W. L.; Lin, Z. *Organometallics* **2003**, *22*, 473−480. (p) Wan, X.; Wang, X.; Luo, Y.; Takami, S.; Kubo, M.; Miyamoto, A. *Organometallics* **2002**, *21*, 3703−3708. (q) Green, A. G.; Liu, P.; Merlic, C. A.; Houk, K. N. *J. Am. Chem. Soc.* **2014**, *136*, 4575−4583. (r) Vanchura, B. A., II; Preshlock, S. M.; Roosen, P. C.; Kallepalli, V. A.; Staples, R. J.; Maleczka, R. E., Jr.; Singleton, D. A.; Smith, M. R., III *Chem. Commun.* **2010**, *46*, 7724−7726 and ref 9j.

(16) (a) Maeda, S.; Morokuma, K. *J. Chem. Phys.* **2010**, *132*, 241102−241104. (b) Maeda, S.; Morokuma, K. *J. Chem. Theory Comput.* **2011**, *7*, 2335−2345. (c) Maeda, S.; Ohno, K.; Morokuma, K. *Phys. Chem. Chem. Phys.* **2013**, *15*, 3683−3701. (d) Maeda, S.; Taketsugu, T.; Morokuma, K. *J. Comput. Chem.* **2014**, *35*, 166−173.

(17) For recent examples of the computational study of unknown organic synthesis reaction mechanisms by the AFIR method, see: (a) Maeda, S.; Komagawa, S.; Uchiyama, M.; Morokuma, K. *Angew. Chem.* **2011**, *123*, 670−675; *Angew. Chem., Int. Ed.* **2011**, *50*, 644−649. (b) Hatanaka, M.; Maeda, S.; Morokuma, K. *J. Chem. Theory Comput.* **2013**, *9*, 2882−2886. (c) Hatanaka, M.; Morokuma, K. *J. Am. Chem. Soc.* **2013**, *135*, 13972−13979. (d) Uematsu, R.; Maeda, S.; Taketsugu, T. *Chem.—Asian J.* **2014**, *9*, 305−312.

(18) (a) Zhao, Y.; Truhlar, D. G. *J. Chem. Phys.* **2008**, *125*, 194101−194118. (b) Zhao, Y.; Truhlar, D. G. *Theor. Chem. Acc.* **2008**, *120*, 215−241.

(19) (a) Cossi, M.; Rega, N.; Scalmani, G.; Barone, V. *J. Comput. Chem.* **2003**, *24*, 669−681. (b) Barone, V.; Cossi, M. *J. Phys. Chem. A* **1998**, *102*, 1995−2001.

(20) In this study, TSs for conformational rearrangements at local minimums were not searched. In the event that a conformation in a local minimum obtained by the IRC calculation in the last step differs from the one for the starting point of the next step, the relative free energy for the lower-energy conformation is shown in the free energy profiles. This treatment assumes that such a conformational rearrangement in local minima occurs easily. In many cases, for qualitative discussions, this assumption is not inappropriate. Actually, the present free energy profiles explain the experimental findings well.

(21) For cation−π interaction, see: (a) Kumpf, R. A.; Dougherty, D. A. *Science* **1993**, *261*, 1708−1710. (b) Dougherty, D. A. *Science* **1996**, *271*, 163−168. (c) Cabarcos, O. M.; Weinheimer, C. J.; Lisy, J. M. *J. Chem. Phys.* **1999**, *110*, 8429−8435. (d) De Wall, S. L.; Barbour, L. J.; Gokel, G. W. *J. Am. Chem. Soc.* **1999**, *121*, 8405−8406. (e) Fukin, G. K.; Lindeman, S. V.; Kochi, J. K. *J. Am. Chem. Soc.* **2002**, *124*, 8329−8336. (f) Forbes, G. C.; Kennedy, A. R.; Mulvey, R. E.; Roberts, B. A.; Rowlings, R. B. *Organometallics* **2002**, *21*, 5115−5121. (g) Lau, J. K-C.; Wong, C. H. S.; Ng, P. S.; Siu, F. M.; Ma, N. L.; Tsang, C. W. *Chem.—Eur. J.* **2003**, *9*, 3383−3396. (h) Siu, F. M.; Ma, N. L.; Tsung, C. W. *Chem.—Eur. J.* **2004**, *10*, 1966−1976. (i) Ruan, C.; Rodgers, M. T. *J. Am. Chem. Soc.* **2004**, *126*, 14600−14610. (j) Ilkhechi, A. H.; Mercero, J. M.; Silanes, I.; Bolte, M.; Scheibitz, M.; Lerner, H.-W.; Ugalde, J. M.; Wargner, M. *J. Am. Chem. Soc.* **2005**, *127*, 10656−10666. (k) Åhman, A.; Nissinen, M. *Chem. Commum.* **2006**, 1209−1211. (l) Davidson, M. G.; Garcia-Vivo, D.; Kennedy, A. R.; Mulvey, R. E.; Robertson, S. D. *Chem.—Eur. J.* **2011**, *17*, 3364−3369. (m) Armstrong, D. R.; Brammer, E.; Cadenbach, T.; Hevia, E.; Kennedy, A. R. *Organometallics* **2013**, *32*, 480−489.

(22) (a) Seeger, R.; Pople, J. A. *J. Chem. Phys.* **1977**, *66*, 3045−3050. (b) Bauernschmitt, R.; Ahlrichs, R. *J. Chem. Phys.* **1996**, *104*, 9047−9052.

(23) Yanai, T.; Tew, D.; Handy, N. *Chem. Phys. Lett.* **2004**, *393*, 51−57.

(24) Iikura, H.; Tsuneda, T.; Yanai, T.; Hirao, K. *J. Chem. Phys.* **2001**, *115*, 3540−3544.

(25) Hudrlik, P. F.; Hudrlik, A. M.; Jeilani, Y. a. *Tetrahedron* **2011**, *67*, 10089−10096.

(26) For the experimental data, see Tables S1 and S2 in the Supporting Information.

(27) Becke, A. D. *J. Chem. Phys.* **1993**, *107*, 8554−8560.

(28) Choi, C.; Elber, R. *J. Chem. Phys.* **1991**, *94*, 751−760.

(29) Stoll, H.; Metz, B.; Dolg, M. *J. Comput. Chem.* **2002**, *23*, 767−778.

(30) Frisch, M. J.; Trucks, G. W.; Schlegel, H. B. et al. Gaussian 09, Revision B.01; Gaussian, Inc.: Wallingford, CT, 2009.

(31) Maeda, S.; Osada, Y.; Morokuma, K.; Ohno, K. *GRRM*, a developmental version; Hokkaido University: Sapporo, Japan.

(32) Suginome, M.; Matsuda, T.; Ito, Y. *Organometallics* **2000**, *19*, 4647−4649.

(33) Lari, A.; Bleiholder, C.; Rominger, F.; Gleiter, R. *Eur. J. Org. Chem.* **2009**, *2009*, 2765−2774.

DOI: 10.1021/ja507675f
J. Am. Chem. Soc. 2015, 137, 4090−4099